USCAP

ARTICLE

Check for updates

Heterogeneity of programmed death-ligand 1 expression and infiltrating lymphocytes in paired resected primary and metastatic non-small cell lung cancer

Jianghua Wu[1,2,3], Wei Sun[1,3], Xin Yang[1], Haiyue Wang[1], Xinying Liu[1], Kaiwen Chi[1], Lixin Zhou[1], Xiaozheng Huang[1], Luning Mao[1], Shuai Zhao[2], Tingting Ding[2], Bin Meng[2] and Dongmei Lin[1]✉

Metastatic tumors (MTs) may show different characteristics of the immune microenvironment from primary tumors (PTs) in non-small cell lung cancer (NSCLC). The heterogeneity of immune markers in metastatic NSCLC and its associated factors has not been well demonstrated. In this study, 64 surgically resected specimens of paired PTs and MTs were obtained from 28 patients with NSCLC. Multiplex immunofluorescence (mIF; panel including programmed death-ligand 1 (PD-L1), Cytokeratin, CD8, and CD68) was performed on whole sections. The heterogeneity of the immune contexture of PD-L1 expression, infiltrating lymphocytes, and immune-to-tumor cell distances was quantified via digital image analysis. In a quantitative comparison of MTs and corresponding PTs, MTs showed higher PD-L1 expression levels, lower density of CD8+ cytotoxic T lymphocytes (CTLs), and longer spatial distance between CTLs and tumor cells. Subgroup analysis, which associated clinical factors, revealed that the heterogeneity of immune markers was more obvious in extrapulmonary, metachronous, and treated MTs, while fewer differences were observed in intrapulmonary, synchronous, and untreated MTs. In particular, MTs showed significantly higher PD-L1 expression and lower lymphocyte infiltration in metastatic NSCLC with EGFR mutations. Prognosis analysis showed that an increased density of CD8+ CTLs in MTs was associated with better overall survival (OS). Therefore, significant discrepancies in PD-L1 expression and lymphocyte infiltration in metastatic NSCLC are most likely associated with temporal heterogeneity with a history of anti-treatment and correlated with EGFR mutations. The detection of immune markers in re-obtained metastatic specimens may be required for immunotherapy prediction in these patients with metastatic NSCLC.

Modern Pathology (2022) 35:218–227; https://doi.org/10.1038/s41379-021-00903-w

INTRODUCTION

Immune checkpoint inhibitors (ICIs) have been approved as first-line and/or second-line treatments for advanced non-small cell lung cancer (NSCLC). The expression of programmed death-ligand 1 (PD-L1) plays a critical role in immune escape mechanisms, and the tumor proportion score (TPS) of PD-L1 expression on tumor cells (TCs) has been widely recommended as a predictive biomarker for ICI immunotherapy in NSCLC [1–3]. In addition, characteristics of immune cells (ICs), such as subtypes, functional polarization, and spatial distribution through the tumor, have also been shown to influence the prognosis of cancer patients and correlate with the response to PD1/PD-L1 target immunotherapy [4, 5].

Based on current detection strategies for immune markers, the response to ICIs is still heterogeneous. Some patients with advanced NSCLC have non-detected metastases at the time of initial diagnosis and eventually develop metastases during the progression of the disease after surgical operation. Patients with metachronous metastases often present with multiple distant metastases, and the majority of them have been managed with systemic treatment, such as tyrosine kinase inhibitors (TKIs), chemotherapy, or radiotherapy (RT) before initiating ICI therapy. Emerging studies have indicated that a therapeutic regimen could affect both PD-L1 expression and characteristics of tumor immune contexture in NSCLC patients receiving neoadjuvant therapy [6–11]. The clinical challenges of tumor heterogeneity in PD-L1 expression and the diversity of immune infiltrates have been a concern in the context of immunotherapy [12–15].

The dynamic evolution of the tumor immune microenvironment (TIME) may occur during tumor metastatic progression. A discrepancy in PD-L1 expression has been noted between a certain proportion of metastatic tumors (MTs) and corresponding primary tumors (PTs) [16–20]. The heterogeneity of TIME of NSCLC in PTs and MTs is vital to address the heterogeneous response of multiple metastases to ICIs. However, the rule of dynamic changes in TIME and its associated clinical factors causing significant metastatic heterogeneity have not been revealed. Research still needs to elucidate what kind of cases may be more likely to exert a significant discrepancy of immune markers in MTs compared to PTs, and it is important to explain under which clinical conditions

[1]Key laboratory of Carcinogenesis and Translational Research (Ministry of Education/Beijing), Department of Pathology, Peking University Cancer Hospital & Institute, Beijing, China. [2]Department of Pathology, Tianjin Medical University Cancer Institute and Hospital; National Clinical Research Center of Cancer; Key Laboratory of Cancer Prevention and Therapy, Tianjin; Tianjin's Clinical Research Center of Cancer, Tianjin, China. [3]These authors contributed equally: Jianghua Wu and Wei Sun. ✉email: Lindm3@163.com

Received: 25 April 2021 Revised: 11 August 2021 Accepted: 12 August 2021
Published online: 7 September 2021

metastatic samples need to be re-obtained for immune markers' detection in patients with metastases. It remains unclear whether this is related to the metastatic sites, time interval, treatment status, or driving genes of metastasis.

Evaluating the tumor immune contexture of MTs in comparison with corresponding PTs may reveal changes in immune markers during NSCLC metastasis. One major challenge is that such studies have been limited by the actual clinical process in which biopsy samples may not show a satisfactory panoramic view of the immune microenvironment, which may result in deviations in the intratumoral heterogeneity between biopsies and surgical specimens [21–23]. In this study, we collected paired surgically resected primary and metastatic samples to avoid potential heterogeneity within the biopsies. We utilized multiplex immunofluorescence (mIF) and digital image analysis to quantitatively identify PD-L1 expression and tumor-infiltrating lymphocytes (TILs) in NSCLC. This study provides beneficial information regarding the heterogeneity of immune markers in metastatic advanced NSCLC and contributes to the current PD-L1 detection strategies.

MATERIALS AND METHODS

Patients and samples

We collected 28 NSCLC cases with available specimens of paired PTs and MTs at Peking University Cancer Hospital and Tianjin Medical University Cancer Hospital from June 2013 to October 2018. The cases were enrolled according to the following criteria: (1) both the PTs and MTs were surgically resected and tissue samples were formalin-fixed paraffin-embedded (FFPE); (2) tumor size was ≥0.5 cm; (3) PTs did not undergo preoperative neoadjuvant treatment; (4) the clinical information and follow-up data were available; and (5) focus was on extrapulmonary distant metastases, but samples of intrapulmonary metastases were also selected as comparative studies. In this study, 64 matched resected specimens were obtained from 28 patients with NSCLC, including eight patients with two resected metastases. Fourteen metastatic samples were intrapulmonary, while 22 metastatic samples were extrapulmonary, including seven brain samples, five adrenal samples, five soft tissue samples (two chest wall samples and three upper limb samples), and five distant lymph node samples.

Histological evaluation

The original histological diagnosis was confirmed in archival hematoxylin and eosin (H&E)-stained slides, and histopathological features, such as histologic subtype and tumor size, were collected. All tumors were pathologically staged according to the TNM classification of the 8th AJCC [24]. Pathological evaluation of multifocal lung cancer was performed using clinical and pathologic criteria, as defined by the International Association for the Study of Lung Cancer (IASLC) Lung Cancer Staging Project to distinguish intrapulmonary metastases from multiple primary lung cancer lesions [25]. All pathologic materials were reviewed by two expert pathologists using the 2015 World Health Organization classification.

Multiplex staining and scanning

Slides were stained with the UltiMapper Kit (Ultivue™ Inc., Cambridge, MA, USA) using the DNA-tagged mIF method. We validated the high comparability of this kit with conventional immunohistochemistry (IHC) of PD-L1 (22c3) and IC quantification in our previous study [26]. Briefly, mIF staining was performed on 4 μm sections of FFPE tissues using BOND RX. FFPE tissue slides were dried at 60–65 °C for 30 min before loading on the BOND RX.

Table 1. Demographics of the included patients and samples.

Total patients ($n = 28$)	**Variables**		**Variables**	
Age (year)	Mean	57.5	Range	52–70
Sex	Male	18	Female	10
Smoker	Yes	17	No	11
Primary tumor				
Location	Right lobe	18	Left lobe	10
AJCC 8th stage	IB-IIB	22	IIIA-IV	6
EGFR	Mutant type	14	Wild type	14
Metastatic tumor	Tumor 1	$n = 28$	Tumor 2	$n = 8$
Metastatic sites	Intrapulmonary	9	Intrapulmonary	5
	Chest wall	2		
	Brain	7		
	Adrenal	3	Adrenal	2
	Soft tissue	3		
	Distant LN	4	Distant LN	1
Time interval	Synchronous	14	Metachronous	22
Adjuvant treatment	With treatment	20	Without treatment	16
	Chem	15		
	Chem + R	1		
	EGFR-TKIs	1		
	Chem + TKIs	3		
Histopathologic type	Primary		Metastases	
	LADC	23	LADC	23
	LSQC	4	LSQC	4
	LCC	1	LCC	1
Survival	Survival	15	Death	13
Follow-up time (days)	Range	335–2603	Median	1364

Chem chemotherapy, *Chem + R* combined chemotherapy and radiotherapy, *EGFR-TKIs* epidermal growth factor receptor tyrosine kinase inhibitors, *Chem + TKIs* combined chemotherapy and EGFR-TKIs, *LN* lymph node, *LADC* lung adenocarcinoma, *LSQC* lung squamous carcinoma, *LCC* large cell carcinoma.

BOND RX was set up for the UltiMapper assay. Five markers were stained simultaneously on one slide using the mIF kit. Reference multiplex images of the UltiMapper® Kit included a panel of PD-L1 (clone 73-10), CD8 (clone C8/144B), CD68 (clone KP-1), cytokeratin (CK, clone AE1/AE3), and 4,6-diamidino-2-phenylindole (DAPI). Digital immunofluorescence images were scanned at 200× magnification in the fluorescent mode. Fluorescent images of DAPI (blue), FITC (CK, Cyan), Cy5 (PD-L1, red) Cy3 (CD8, green), and Cy7 (CD68, orange) for each section were captured in the corresponding channels.

Quantified analysis of multiplex images

The digital images were analyzed using HALO™ software (version 3.0; Indica Labs, Corrales, NM, USA). Before the analysis, the tumor areas were annotated in each digital whole-slide image. The intratumoral cell populations and densities for the phenotypes of interest (PD-L1+ cells, CK+ TCs, CD8+ cytotoxic T lymphocytes (CTLs), CD68+ macrophages, and PD-L1+/CK+ double-positive phenotype) were counted within the tumor area. TPS was quantitatively calculated as the proportion of intratumoral PD-L1+/CK+ TCs and CK+ TCs (Fig. S1). In addition to cell populations, digital image analysis on mIF enabled the localization of individual cells across whole sections, and subsequently determined the spatial distance of each type of IC with respect to adjacent TCs. Digital images were analyzed with cell segmentation to identify stained cells and map their *x*–*y* coordinates. The cell data are plotted, and then the *x*–*y* coordinates are used to quantify the average distance between the ICs and adjacent TCs using the proximity algorithm in HALO system (Fig. S2).

Statistical analysis

The Wilcoxon signed-rank test was used for the quantitative comparison of paired PTs and MTs, and the Mann–Whitney test was used for non-paired PTs and MTs. Cohen's κ coefficient of agreement was evaluated using the dichotomized TPS, and the value of κ was categorized as poor (<0.40), moderate (0.40–0.8), or excellent (≥0.8). Kaplan–Meier curves were used to assess the impact of biomarkers on overall survival (OS). The significance of biomarkers was determined by univariate and multivariate analyses using the log-rank test and Cox proportional hazards models. Statistical significance was set at $p < 0.05$. Statistical analyses were performed using SPSS Statistics software, version 22 (IBM Corp., Armonk, NY, USA).

RESULTS

Patient demographics and clinicopathological characteristics

The characteristics of the 28 patients with NSCLC are summarized in Table 1. The median age was 57.5 years (range: 52–70 years); 18 patients were men and 10 were women. Smokers accounted for 60.71% (17/28) of the participants. Twenty-two patients were in AJCC 8th stage IB-IIB at the first surgical operation, while six patients were at stage IIIA-IV. Metachronous metastases were defined based on the time interval between tumor lesions of more than 6 months after the diagnosis. In our study, patients developed both synchronous metastases (14 samples) and metachronous metastases (22 samples). Among the collected metastatic samples, 16 samples were not treated, while 20 out of 22 metachronous metastases samples were subjected to anti-tumor treatments. Pathologic examination revealed that lung adenocarcinoma (LADC, 23/28, 82.1%) was the major histological type. Squamous carcinoma (LSQC, 4/28, 14.3%) and large cell carcinoma (LCC, 1/28, 3.6%) were also confirmed. Fourteen of 28 cases (50%) were found to harbor an *EGFR* mutant, and the remaining 14 cases were *EGFR* wild-type. None of the cases harbored ALK or ROS-1 rearrangements. The follow-up time ranged from 335 to 2603 days, with a median of 1364 days. Thirteen patients died during the follow-up period due to lung cancer.

Heterogeneity of PD-L1 expression and TILs in primary and metastatic NSCLC

Representative images of mIF stains of each cell subset in primary and metastatic NSCLC tumors are shown in Fig. 1A. We first

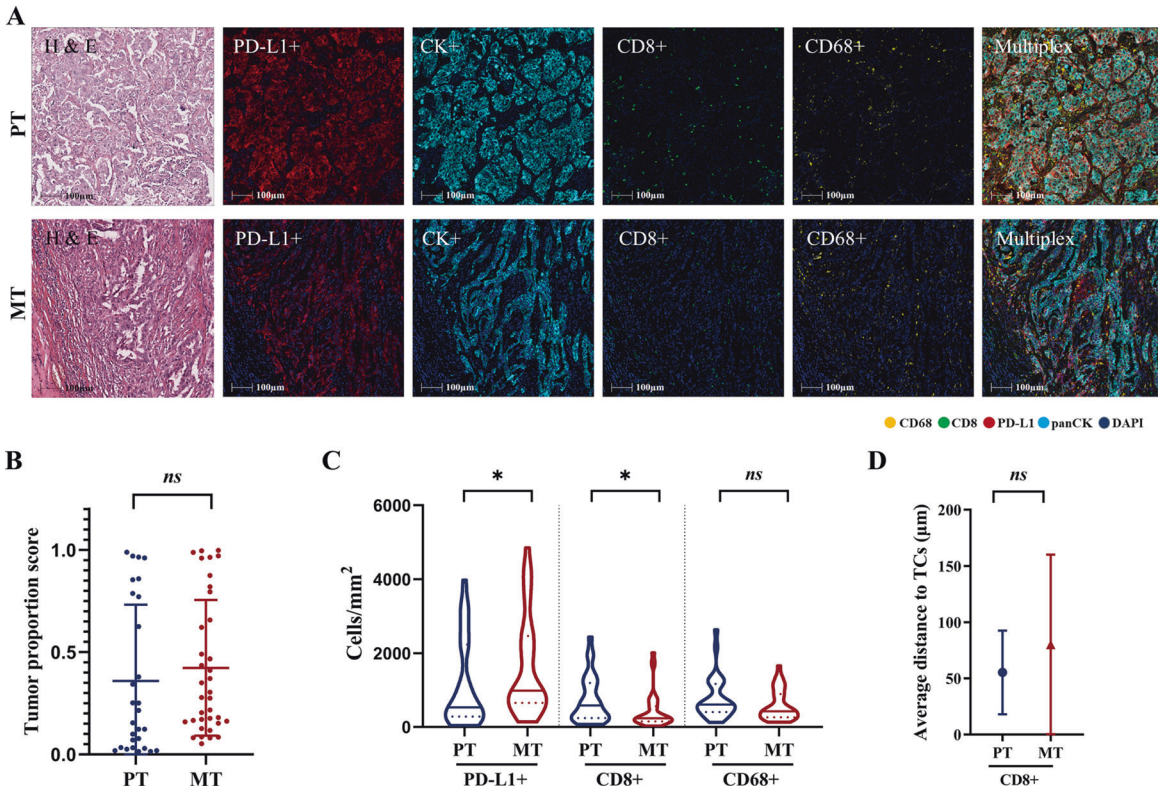

Fig. 1 Multiplex immunofluorescence (mIF) staining on immune markers in primary and metastatic tumors. A The represented images of mIF staining on PD-L1 expression, tumor cells (TCs), and immune cells (ICs) in primary tumors (PTs) and metastatic tumors (MTs). Comparison the tumor proportion score of PD-L1 expression (**B**), ICs infiltration (**C**), and immune-to-tumor cell distances (**D**) in non-paired PTs and MTs, Mann–Whitney test.

Table 2. Heterogeneity of PD-L1 expression, lymphocytes infiltration and immune-to-tumor cell distances between primary and metastatic samples in non-small cell lung cancer.

Immune markers	Heterogeneity		Paired	Non-paired
	PT	MT	p^a	p^b
TPS (average, score %)	35.91%	42.34%	0.046*	0.096
PD-L1+ (average, cell/mm^2)	859.63	1391.86	0.029*	0.042*
CD8+ (average, cell/mm^2)	736.90	436.75	0.040*	0.022*
CD68+ (average, cell/mm^2)	776.18	592.01	0.068	0.102
CD8+ to TCs (average, μm)	55.24	80.26	0.038*	0.304
CD68+ to TCs (average, μm)	41.62	46.68	0.285	0.507

[a]Wilcoxon signed-rank test.
[b]Mann–Whitney test; *$p < 0.05$, considered statistically significant. *PT* primary tumor, *MT* metastatic tumor, *TPS* tumor proportion score, *TCs* tumor cells.

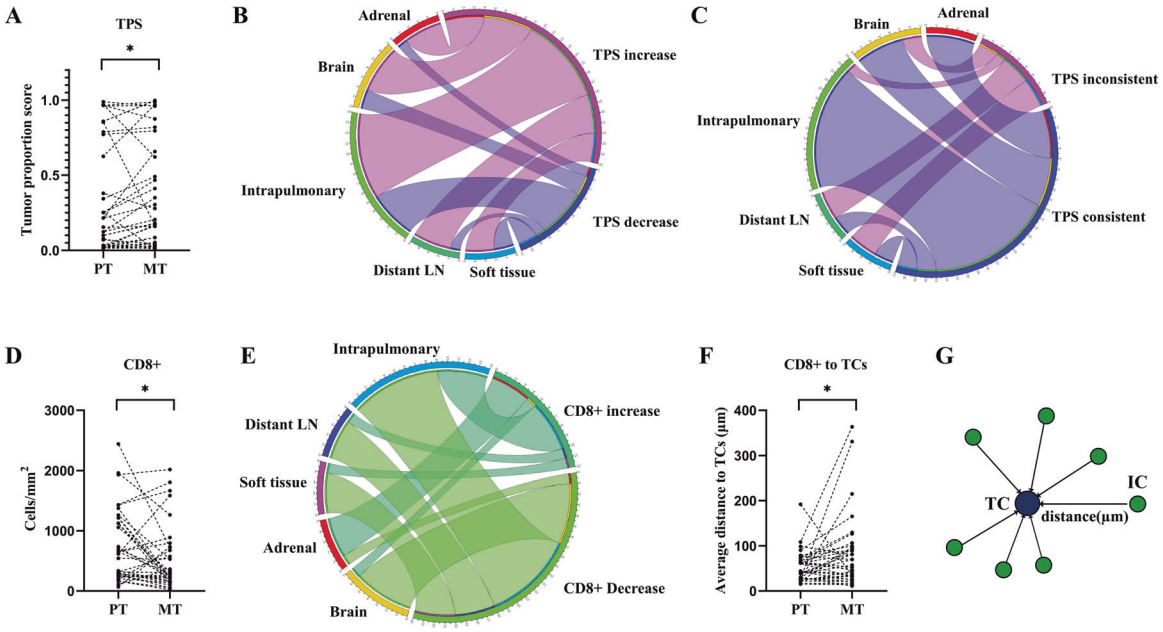

Fig. 2 Heterogeneity of immune markers in paired primary and metastatic tumors. A Heterogeneity in the tumor proportion score (TPS) of PD-L1 expression between paired primary tumors (PTs) and metastatic tumors (MTs). **B** Circos figure shows the increase and decrease in the continuous quantified value of TPS in different sites of metastases. **C** Circos figure shows the agreements of categorical TPS in MTs. **D** Heterogeneity in CD8+ cytotoxic T lymphocytes (CTLs) infiltration between paired PTs and MTs. **E** Circos figure shows the increase and decrease of CTLs infiltrating in MTs. **F** Heterogeneity in the spatial distance of CTLs and tumor cells (TCs) between paired PTs and MTs. **G** Schematic diagram illustrates the spatial distribution of the immune-to-tumor cell distances.

compared PD-L1 expression and infiltrating lymphocytes in non-paired PTs and MTs using the Mann–Whitney test (Table 2). The results showed that MTs generally had a higher PD-L1 expression level in PD-L1+ cell populations ($p = 0.042$) and a higher TPS (median: 29.16% vs. 18.50%; average: 42.34% vs. 35.91%, $p = 0.096$) (Fig. 1B). A lower density of CD8+ CTLs ($p = 0.022$) in MTs was statistically significant (Fig. 1C), but no statistical discrepancies in the spatial distance of ICs to TCs were found (Fig. 1D).

The heterogeneity of the quantitative immune markers between paired PTs and MTs was identified using the Wilcoxon signed-rank test (Table 2). Generally, paired PTs and MTs showed a significant change in the density of PD-L1+ cells ($p = 0.029$) and a significant heterogeneity in TPS ($p = 0.046$) (Fig. 2A). Among all 36 paired samples of 28 patients, 25 paired samples demonstrated an increase in TPS, only 11 paired samples showed a decrease in TPS in MTs compared with PTs (Fig. 2B). Dichotomizing the samples using cutoffs of 5% and 50%, respectively, TPS was consistent in the 28 paired lesions (77.8%) and inconsistent in eight samples (22.2%). A moderate agreement of TPS was achieved ($\kappa = 0.448$) at a cutoff of 5%, while an excellent agreement of TPS was observed at a cutoff of 50% ($\kappa = 0.869$) (Fig. 2C and Table S1).

MTs showed significant changes in the density of CD8+ CTLs ($p = 0.040$), but this was not statistically significant for CD68+ macrophages ($p = 0.068$) (Fig. 2D). More paired MT samples showed a decrease in the density of ICs, while a few cases showed an increase in IC infiltrates (Fig. 2E). The spatial relationship was analyzed in paired PTs and MTs, and the results showed that the average spatial distance between CD8+ CTLs and TCs was significantly longer in MTs than in PTs ($p = 0.038$) (Fig. 2F, G).

Spatial heterogeneity of PD-L1 expression and TILs in primary and metastatic NSCLC

In addition to the total samples, the spatial heterogeneity of immune contexture in paired primary and metastatic NSCLC was analyzed to show the possible discrepancies in different locations of metastases. Subgroups of extrapulmonary MT (eMT) and intrapulmonary MT (iMT) were compared (Fig. 3 and Table S2). In paired eMTs and corresponding PTs, the changes in the density

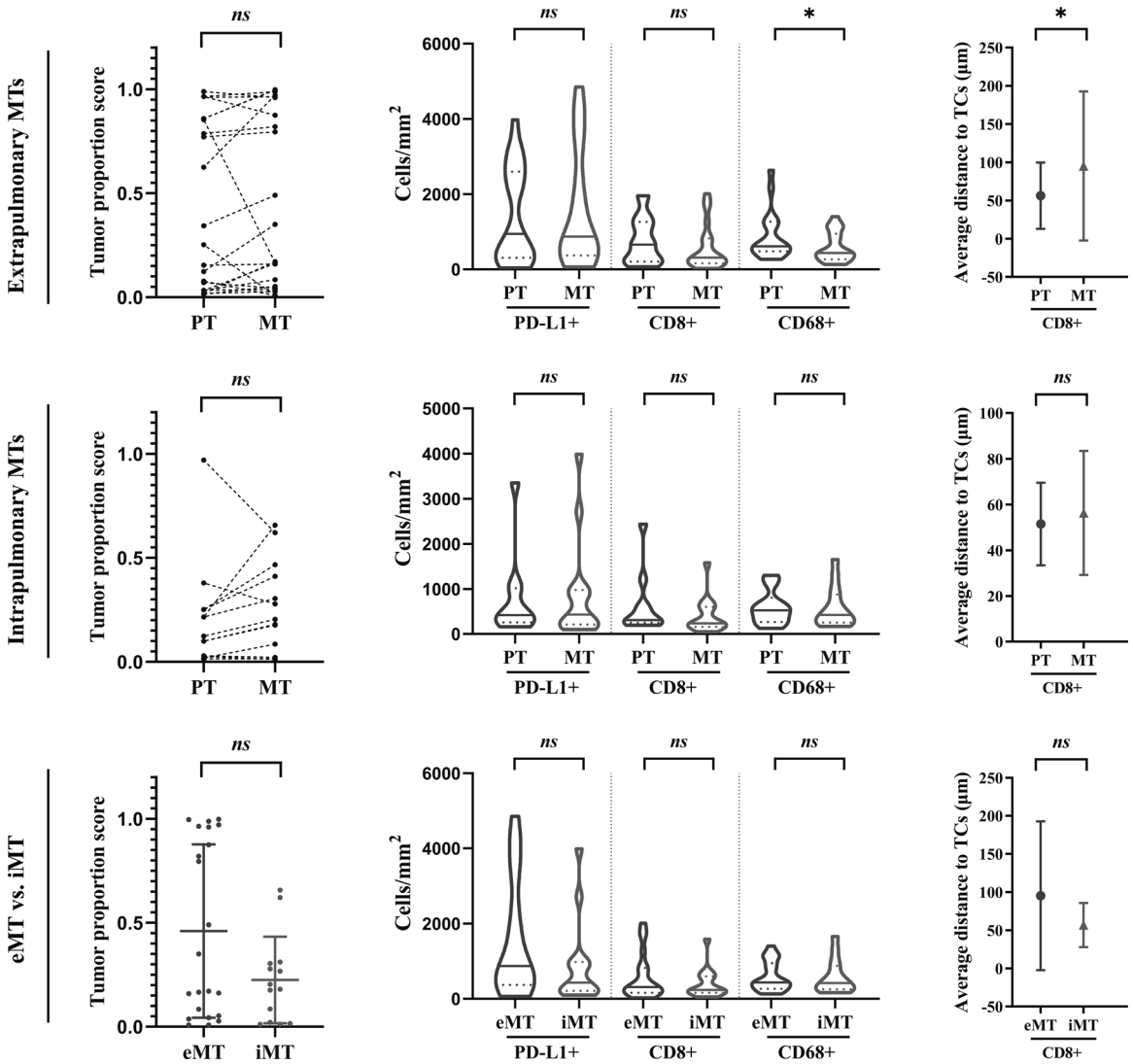

Fig. 3 Spatial heterogeneity of immune markers in metastatic tumors. The heterogeneity of PD-L1 expression, immune cell infiltration, and immune-to-tumor cell distances in subgroups of extrapulmonary metastatic tumors (eMTs) and intrapulmonary metastatic tumors (iMTs).

of PD-L1+ cells and TPS were not significant (both $p > 0.05$), while immune infiltrates decreased in most samples, with significant discrepancies in the density of CD68+ cells ($p = 0.039$). A significant increase in the average distance between CD8+ CTLs and TCs was also observed ($p = 0.046$). In contrast, in paired iMTs and corresponding PTs, significant discordance was not observed in PD-L1 expression, infiltrating lymphocytes, or spatial relations between ICs and TCs.

As for TPS with dichotomized results at a cutoff of 5%, there was poor agreement in paired eMTs ($\kappa = 0.154$), whereas there was good agreement in paired iMTs ($\kappa = 0.837$). At a cutoff of 50%, a high agreement of TPS was observed ($\kappa \geq 0.8$) in both subgroups of eMTs and iMTs (Table S1).

We also compared PD-L1 expression and infiltrating lymphocytes between eMT and iMT samples, and no significant discrepancies were observed.

Temporal heterogeneity of PD-L1 expression and TILs in primary and metastatic NSCLC

The heterogeneity of immune contexture in metachronous MT (mMT) and synchronous MT (sMT) in NSCLC was analyzed (Fig. 4 and Table S3). In paired mMTs and corresponding PTs, the heterogeneity of the density of PD-L1+ cells, and the changes in TPS were not significant, while IC populations decreased in most samples with significant discrepancies in the density of CD8+ ($p = 0.008$) and CD68+ ($p = 0.003$). A significant increase in the average distance of CD8+ ICs and CD68+ ICs to TCs was observed ($p = 0.003$ and $p = 0.024$, respectively). In contrast, in paired sMTs and corresponding PTs, no significant discrepancies were observed.

As for TPS with dichotomized results at a cutoff of 5%, there was poor agreement in paired mMTs ($\kappa = 0.304$), whereas there was moderate agreement in paired sMTs ($\kappa = 0.553$). At a cutoff of 50%, a high agreement of TPS was observed ($\kappa \geq 0.8$) in both subgroups of mMTs and sMTs (Table S1).

We compared PD-L1 expression and infiltrating lymphocytes between the mMT and sMT subgroups. Significant differences were not observed in PD-L1 expression and immune infiltrates, while a longer average distance of CD8+ ICs to TCs was found in mMTs ($p = 0.011$).

Heterogeneity of PD-L1 expression and TILs in treated and untreated metastatic NSCLC

To assess the possible impact of postoperative adjuvant treatment on MTs, the heterogeneity of immune contexture in treated MT (tMT) and untreated MT (uMT) was analyzed (Fig. 5 and Table S4). In paired tMTs and corresponding PTs, significant heterogeneity

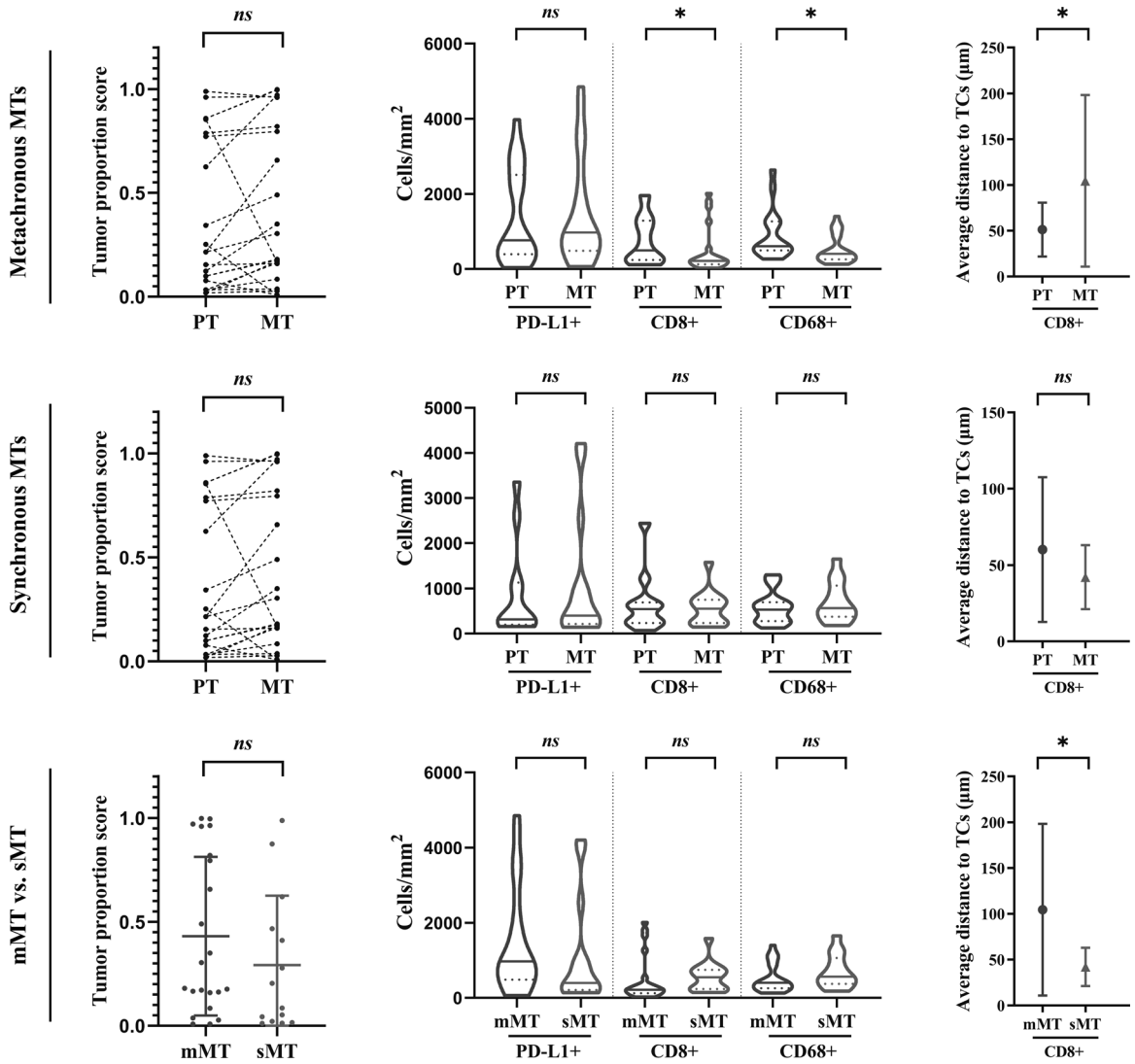

Fig. 4 Temporal heterogeneity of immune markers in metastatic tumors. The heterogeneity of PD-L1 expression, immune cell infiltration, and immune-to-tumor cell distances in subgroups of metachronous metastatic tumors (mMTs) and synchronous metastatic tumors (sMTs).

with a higher density was observed in PD-L1+ cells ($p = 0.047$) and changes in TPS ($p = 0.040$). Most samples showed a decrease in cell populations with significant discrepancies in the density of CD8+ ($p = 0.019$) and CD68+ ($p = 0.001$) ICs. A significant increase in the average distance of CD8+ and CD68+ ICs to TCs was also observed ($p = 0.004$ and $p = 0.017$, respectively). In contrast, in paired uMTs and the corresponding PTs, no significant discrepancies were observed.

As for TPS with dichotomized results at a cutoff of 5%, there was poor agreement in paired tMTs ($\kappa = 0.216$), whereas there was moderate agreement in paired uMTs ($\kappa = 0.500$). At a cutoff of 50%, a moderate agreement was observed in tMTs ($\kappa = 0.792$), while a high agreement of TPS was observed in uMTs (Table S1).

PD-L1 expression and infiltrating lymphocytes between the tMT and uMT subgroups were compared. A higher density of PD-L1+ cells ($p = 0.013$) and higher TPS ($p = 0.033$) were observed in tMTs. A longer average distance of CD8+ ICs to TCs was also found in tMTs than in uMTs ($p = 0.014$).

Heterogeneity of PD-L1 expression and TILs in EGFR-mutated primary and metastatic NSCLC

The heterogeneity of immune contexture between primary and metastatic NSCLC cases was analyzed according to EGFR mutation status (Fig. 6 and Table S5). In the EGFR-mutant subgroup, significant heterogeneity with a higher density of PD-L1+ cells ($p = 0.004$) and an increase in TPS ($p = 0.002$) were observed in paired MTs and corresponding PTs. Most samples showed a decrease in cell populations with significant discrepancies in the density of CD8+ ICs ($p = 0.006$). A significant increase in the average distance of CD8+ ICs to TCs was also observed ($p = 0.019$). In contrast, in the EGFR-wild subgroup, no significant discrepancies in immune markers were observed in the paired MTs and corresponding PTs.

As for TPS with dichotomized results at a cutoff of 5%, there was poor agreement in paired MTs in EGFR-mutant cases ($\kappa = 0.271$), whereas there was an obvious higher agreement in paired MTs in EGFR-wild cases ($\kappa = 0.765$). At a cutoff of 50%, a moderate agreement was observed in EGFR-mutant cases ($\kappa = 0.773$), while a high agreement of TPS was observed in EGFR-wild cases ($\kappa = 0.875$) (Table S1).

Prognostic significance of the immune biomarkers in metastatic NSCLC

We analyzed the correlations between immune markers and OS in PTs and MTs separately. In PTs, none of the immune markers significantly correlated with OS, while in MTs, a higher density

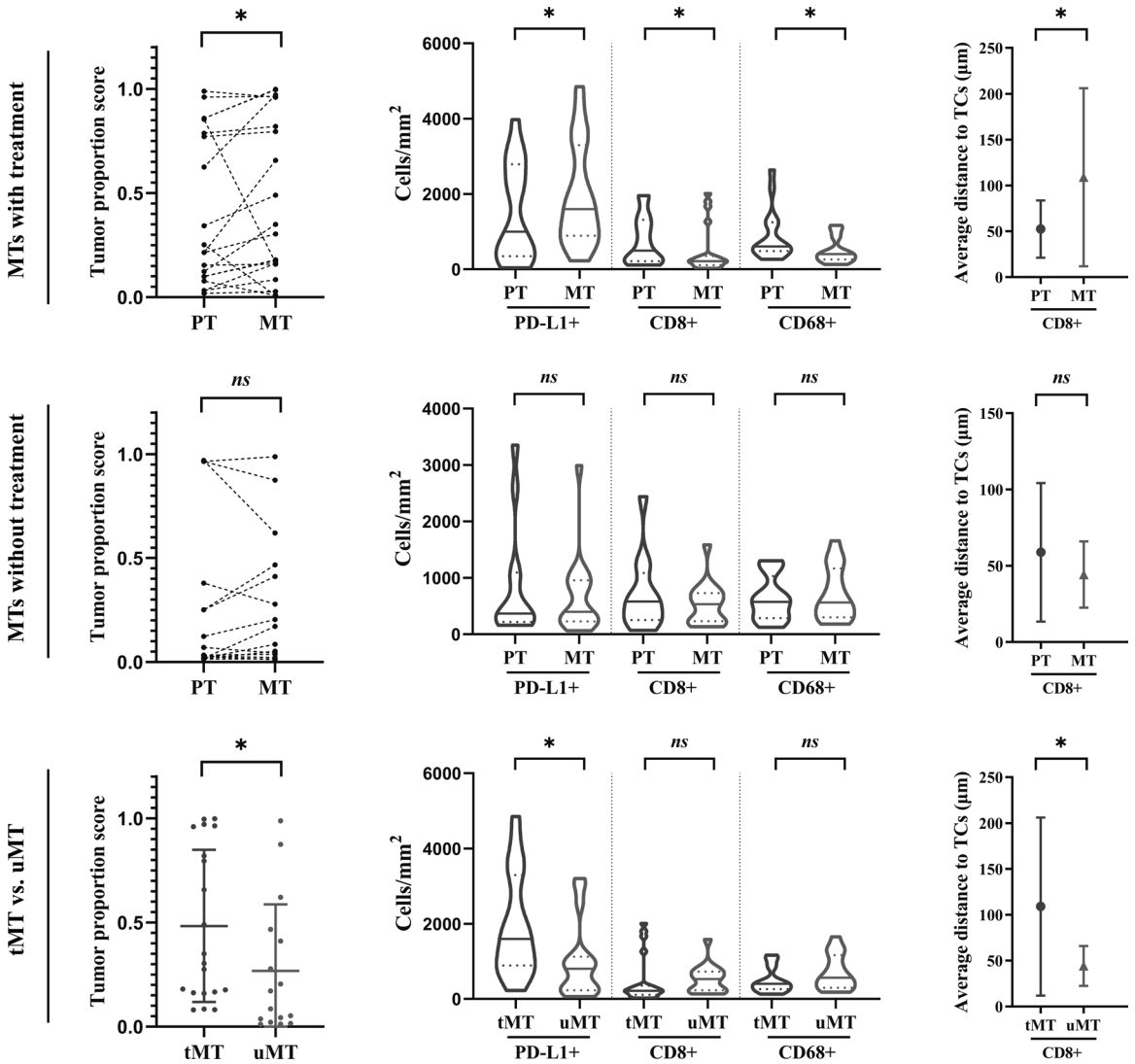

Fig. 5 Heterogeneity of immune markers according to treatment status. The heterogeneity of PD-L1 expression, immune cell infiltration, and immune-to-tumor cell distances in subgroups of treated metastatic tumors (tMTs) and untreated metastatic tumors (uMTs).

(higher than the median) of CD8+ CTLs significantly correlated with a better outcome ($p = 0.0183$). In particular, we compared the change in status (decrease or increase) of the quantitative immune markers in MTs compared to PTs. Our results showed that an increase in TPS was marginally correlated with a poor outcome ($p = 0.0625$), while an increase in the density of CD8+ cells ($p = 0.0273$) was significantly correlated with a better outcome. Multivariate analyses incorporating clinical parameters revealed that an increase in CD8+ ICs in MTs compared to corresponding PTs was an independent factor associated with a low risk of cancer-related death in metastatic NSCLC ($p = 0.0385$, hazard risk (HR): 0.1151, 95% CI [0.0149–0.8917]) (Fig. 7 and Table S6).

DISCUSSION

The evolution of TIME and the intertumoral heterogeneity of immune markers in MTs are a concern in immunotherapy practice. In this study, we demonstrated the quantitative heterogeneity of immune contexture, including PD-L1 expression, lymphocyte infiltrates, and spatial relations between ICs and TCs in surgically derived whole sections of NSCLC via digital image analysis. We also revealed the possible factors associated with significant heterogeneity.

The TPS of PD-L1 expression is widely used to predict the response to PD1/PD-L1 inhibitors in advanced NSCLC. The inconsistency of TPS in a proportion of metastatic NSCLC has been reported, this may be due to the sample selection, intratumoral heterogeneity of biopsy samples, and inter-variability among observers [16–20]. Accurate assessment of PD-L1 scoring is a major challenge for pathologists, and only semi-quantitative scores can be evaluated on current IHC slides. Compared with conventional IHC, digital mIF images enable multiplexed, quantitative analysis of tissue specimens for co-expressed PD-L1 on TCs and ICs. Thus, a digital mIF image method enables the quantitative assessment of TPS discrepancies between MTs and PTs.

Our quantitative results of TPS on surgically resected samples showed that significant heterogeneity of PD-L1 expression was observed in MTs compared to corresponding PTs, and more cases showed a higher level of PD-L1+ cell populations with an increased TPS, suggesting that PD-L1 expression is more commonly increased in metastatic NSCLC. The ATLANTIC trial reported that the expression of PD-L1 was significantly higher in tumor samples that received chemotherapy or radiotherapy before sampling than in tumor samples that did not receive treatment [27]. Similarly, we used paired samples and observed higher PD-L1 expression mainly in treated MT samples, suggesting

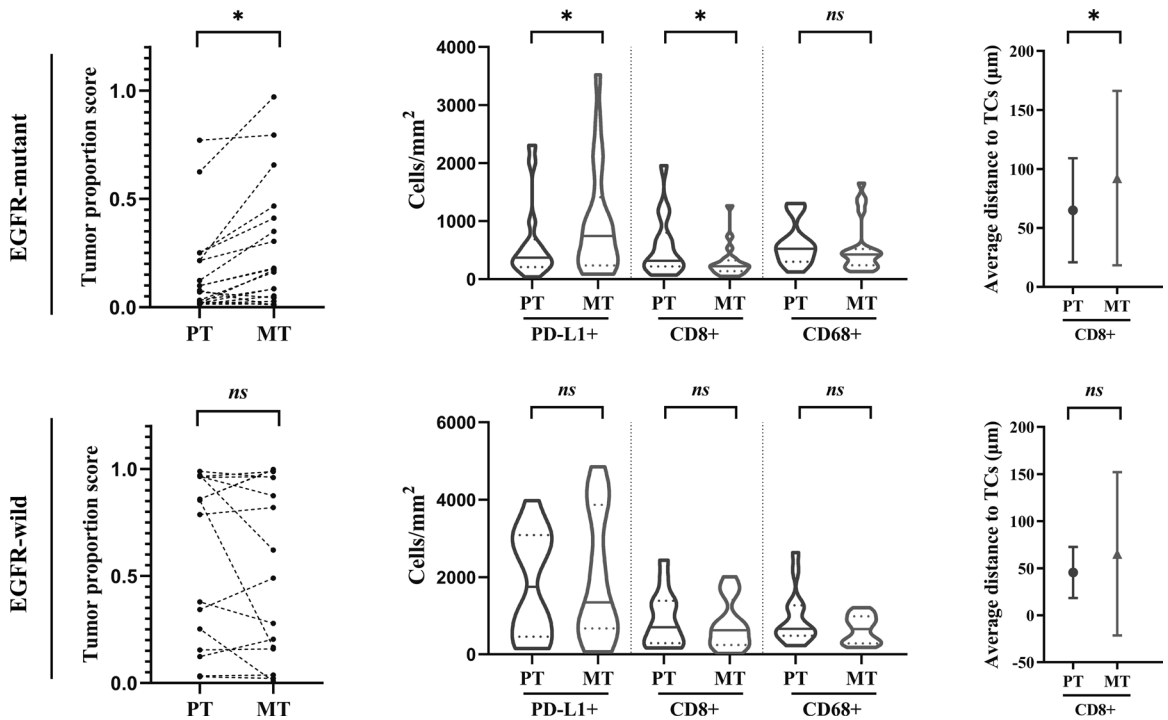

Fig. 6 Heterogeneity of immune markers according to EGFR mutation status. The heterogeneity of PD-L1 expression, immune cell infiltration, and immune-to-tumor cell distances according to EGFR mutation status in non-small cell lung cancer.

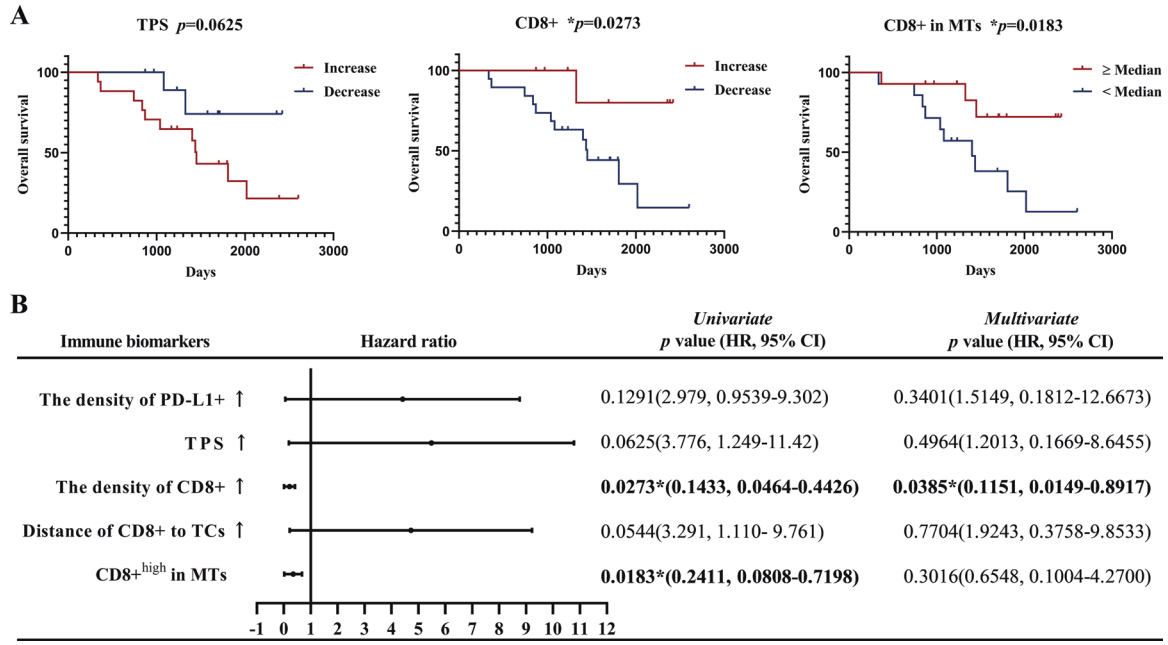

Fig. 7 Prognostic significance of immune biomarkers in metastatic tumors. A Survival analysis of immune biomarkers in metastatic tumors (MTs) and its change status with overall survival (OS). **B** Forest tree showing the risk of the heterogeneity of immune markers in metastatic NSCLC.

that PD-L1 expression more commonly increased in metastases with a history of traditional anti-tumor treatment than in samples with natural tumor progression. This is helpful for the immunotherapy strategy of following clinical treatment in patients with NSCLC who develop distant metastases.

The characteristics of the immune microenvironment play a vital role in anticancer immunity. Mansfield et al. reported that brain metastases may lack either PD-L1 expression, lymphocyte infiltration, or both, in contrast to primary lung cancer samples [28]. In our cohort of paired samples, most MTs had lower CD8+ CTL infiltrates with varying degrees, indicating that most MTs possibly have a lower ability to recruit ICs against TCs after metastatic progression, especially in distant metastases. In addition, the multiplex strategy enabled us to provide an in situ map with spatial cell distribution. A closer spatial distance between ICs and TCs is commonly considered as a possible

effective immune-to-tumor cell interaction [29–31]. Therefore, an increase in the spatial distance between infiltrating CD8+ cells and TCs in MTs indicated that the role of CTLs in TCs possibly decreased in most metastases.

Since advanced-NSCLC patients commonly develop several distant metastases, there is clinical confusion regarding the use of primary lesions or metastases for detecting immune markers. Exploring the main clinical factors causing the significant heterogeneity of immune markers in metastatic NSCLC may be helpful in addressing this challenge. Subgroup analysis of the associated clinical factors showed that the discrepancies in PD-L1 expression and TILs were mainly observed in subgroups of extrapulmonary, metachronous, and treated MTs, but not for intrapulmonary, synchronous, and untreated MTs. In particular, postoperative adjuvant therapy had a significant influence on tumor immune markers (Fig. S3). These results are consistent with those of a study on brain metastases in which the time is associated with CD8 expression discordance [32]. This means that in patients who developed metachronous MTs with adjuvant treatment, the MTs are suggested to be re-obtained for the detection of immune biomarkers as a significant change in comparison with PTs. It is important to predict the heterogeneous response of ICIs to multiple distant metastases in patients with advanced disease. In contrast, for intrapulmonary and synchronous metastasis, both PTs and MTs are suitable for the detection of immune markers.

EGFR mutation is the most common driver gene in East Asian NSCLC patients and is usually negatively correlated with PD-L1 expression [33]. Studies have shown that NSCLC patients with EGFR mutations commonly have a poor response to ICI immunotherapy [34–38]. We evaluated immune biomarkers in EGFR-mutant and wild-type NSCLC cases. Interestingly, we observed significant heterogeneity of immune contexture only in EGFR-mutant NSCLC, and nearly most samples showed an increase in PD-L1 score in paired MTs in the EGFR-mutant subgroup. The activation of the EGFR signaling pathway in NSCLC may upregulate the expression of PD-L1 and immunosuppressive factors, thereby promoting the immunosuppressive effect in TIME. Analyzing the mechanism of EGFR in the regulation of PD-L1 expression during NSCLC metastatic progression may be of interest in future research.

In this cohort, an increase in immune infiltrates was correlated with a better outcome. Similarly, Camy et al. found that CD8 expression in brain MTs was marginally associated with a better prognosis for brain metastatic lung cancer [32]. Considering the role of immunomodulation in tumor progression, the changing status of lCs may represent a positive or negative trend in the immune response, and an increase in the density of CTLs in MTs predicts a better outcome. Thus, when samples of both MTs and PTs are available, detection and comparison of changes in the status of immune infiltrates may be clinically useful for predicting the OS in patients with metastatic NSCLC.

Our study has some limitations. The major drawback of this study was the small number of samples, because the resected samples were unusual in patients with distant metastases. Some subgroup analyses on clinical factors, such as the impact of different therapies, were not performed. The impact of clinical factors on the heterogeneity of immune markers requires a larger sample size to be verified. In addition, the impact of the heterogeneity of immune markers in response to immunotherapy remains to be investigated in subsequent studies.

In conclusion, there was heterogeneity in PD-L1 expression and infiltrating lymphocytes between primary and metastatic NSCLC samples. Significant discrepancies were mainly observed in long-term metastases with a history of traditional adjuvant treatment and were correlated with EGFR mutations. MTs in these patients are recommended to be re-obtained as predictive samples because of the significant heterogeneity of immune biomarkers from PTs. In future studies, whether the heterogeneity of PD-L1 expression and TILs during NSCLC metastasis exerts an impact on the heterogeneous response to immunotherapy needs further verification.

DATA AVAILABILITY

The datasets generated and/or analyzed during the current study are available from the corresponding author upon reasonable request.

REFERENCES

1. Dong, H. et al. Tumor-associated B7-H1 promotes T-cell apoptosis: a potential mechanism of immune evasion. *Nat. Med.* **8**, 793–800 (2002).
2. Tumeh, P. C. et al. PD-1 blockade induces responses by inhibiting adaptive immune resistance. *Nature* **515**, 568–571 (2014).
3. Lantuejoul, S. et al. PD-L1 testing for lung cancer in 2019: perspective from the IASLC pathology committee. *J. Thorac. Oncol.* **15**, 499–519 (2020).
4. Blank, C. U., Haanen, J. B., Ribas, A. & Schumacher, T. N. CANCER IMMUNOLOGY. The "cancer immunogram". *Science* **352**, 658–660 (2016).
5. Binnewies, M. et al. Understanding the tumor immune microenvironment (TIME) for effective therapy. *Nat. Med.* **24**, 541–550 (2018).
6. Parra, E.R. et al. Effect of neoadjuvant chemotherapy on the immune microenvironment in non-small cell lung carcinomas as determined by multiplex immunofluorescence and image analysis approaches. *J. Immunother. Cancer* **6**, 48 (2018).
7. Zhang, P. P. et al. Upregulation of programmed cell death ligand 1 promotes resistance response in non-small-cell lung cancer patients treated with neoadjuvant chemotherapy. *Cancer Sci.* **107**, 1563–1571 (2016).
8. Han, J. J. et al. Change in PD-L1 expression after acquiring resistance to Gefitinib in EGFR-mutant non-small-cell lung cancer. *Clin. Lung Cancer* **17**, 263–270.e2 (2016).
9. Kang, T. H. et al. Chemotherapy acts as an adjuvant to convert the tumor microenvironment into a highly permissive state for vaccination-induced antitumor immunity. *Cancer Res.* **73**, 2493–2504 (2013).
10. Remark, R. et al. Immune contexture and histological response after neoadjuvant chemotherapy predict clinical outcome of lung cancer patients. *Oncoimmunology* **5**, e1255394 (2016).
11. Song, Z., Yu, X. & Zhang, Y. Altered expression of programmed death-ligand 1 after neo-adjuvant chemotherapy in patients with lung squamous cell carcinoma. *Lung Cancer* **99**, 166–171 (2016).
12. Riaz, N. et al. Tumor and microenvironment evolution during immunotherapy with Nivolumab. *Cell* **171**, 934–949.e16 (2017).
13. Junttila, M. R. & de Sauvage, F. J. Influence of tumour micro-environment heterogeneity on therapeutic response. *Nature* **501**, 346–354 (2013).
14. Jimenez-Sanchez, A. et al. Heterogeneous tumor-immune microenvironments among differentially growing metastases in an ovarian cancer patient. *Cell* **170**, 927–938.e20 (2017).
15. Van den Eynde, M. et al. The link between the multiverse of immune microenvironments in metastases and the survival of colorectal cancer patients. *Cancer Cell* **34**, 1012–1026.e3 (2018).
16. Pinato, D. J. et al. Intra-tumoral heterogeneity in the expression of programmed-death (PD) ligands in isogeneic primary and metastatic lung cancer: implications for immunotherapy. *Oncoimmunology* **5**, e1213934 (2016).
17. Takamori, S. et al. Discrepancy in programmed cell death-ligand 1 between primary and metastatic non-small cell lung cancer. *Anticancer Res.* **37**, 4223–4228 (2017).
18. Uruga, H. et al. Programmed cell death ligand (PD-L1) expression in stage II and III lung adenocarcinomas and nodal metastases. *J. Thorac. Oncol.* **12**, 458–466 (2017).
19. Keller, M. D. et al. Adverse prognostic value of PD-L1 expression in primary resected pulmonary squamous cell carcinomas and paired mediastinal lymph node metastases. *Mod. Pathol.* **31**, 101–110 (2018).
20. Cho, J. H. et al. Programmed death ligand 1 expression in paired non-small cell lung cancer tumor samples. *Clin. Lung Cancer* **18**, e473–e479 (2017).
21. Gniadek, T. J. et al. Heterogeneous expression of PD-L1 in pulmonary squamous cell carcinoma and adenocarcinoma: implications for assessment by small biopsy. *Mod. Pathol.* **30**, 530–538 (2017).
22. Li, C. et al. Comparison of 22C3 PD-L1 expression between surgically resected specimens and paired tissue microarrays in non-small cell lung cancer. *J. Thorac. Oncol.* **12**, 1536–1543 (2017).
23. Gagne, A. et al. Comprehensive assessment of PD-L1 staining heterogeneity in pulmonary adenocarcinomas using tissue microarrays: impact of the architecture pattern and the number of cores. *Am. J. Surg. Pathol.* **42**, 687–694 (2018).

24. Goldstraw, P. et al. The IASLC Lung Cancer Staging Project: proposals for revision of the TNM stage groupings in the forthcoming (eighth) edition of the TNM Classification for Lung Cancer. *J. Thorac. Oncol.* **11**, 39–51 (2016).
25. Travis, W. D. et al. International Association for the Study of Lung Cancer/American Thoracic Society/European Respiratory Society International Multidisciplinary Classification of Lung Adenocarcinoma. *J. Thorac. Oncol.* **6**, 244–285 (2011).
26. Wu, J. et al. Validation of multiplex immunofluorescence and digital image analysis for programmed death-ligand 1 expression and immune cell assessment in non-small cell lung cancer: comparison with conventional immunohistochemistry. *J. Clin. Pathol.* https://doi.org/10.1136/jclinpath-2021-207448 (2021).
27. Boothman, A. M. et al. Impact of patient characteristics, prior therapy, and sample type on tumor cell programmed cell death ligand 1 expression in patients with advanced NSCLC screened for the ATLANTIC Study. *J. Thorac. Oncol.* **14**, 1390–1399 (2019).
28. Mansfield, A. S. et al. Temporal and spatial discordance of programmed cell death-ligand 1 expression and lymphocyte tumor infiltration between paired primary lesions and brain metastases in lung cancer. *Ann. Oncol.* **27**, 1953–1958 (2016).
29. Carstens, J. L. et al. Spatial computation of intratumoral T cells correlates with survival of patients with pancreatic cancer. *Nat. Commun.* **8**, 15095 (2017).
30. Feng, Z. et al. Multiparametric immune profiling in HPV^{-} oral squamous cell cancer. *JCI Insight* **2**, e93652 (2017).
31. Joshi, K. et al. Spatial heterogeneity of the T cell receptor repertoire reflects the mutational landscape in lung cancer. *Nat. Med.* **25**, 1549–1559 (2019).
32. Camy, F. et al. Brain metastasis PD-L1 and CD8 expression is dependent on primary tumor type and its PD-L1 and CD8 status. *J. Immunother. Cancer* **8**, e000597. (2020).
33. Wu, J. et al. The correlation and overlaps between PD-L1 expression and classical genomic aberrations in Chinese lung adenocarcinoma patients: a single center case series. *Cancer. Biol. Med.* **16**, 811–821 (2019).
34. Rittmeyer, A. et al. Atezolizumab versus docetaxel in patients with previously treated non-small-cell lung cancer (OAK): a phase 3, open-label, multicentre randomised controlled trial. *Lancet* **389**, 255–265 (2017).
35. Peters, S. et al. Phase II trial of Atezolizumab as first-line or subsequent therapy for patients with programmed death-ligand 1-selected advanced non-small-cell lung cancer (BIRCH). *J. Clin. Oncol.* **35**, 2781–2789 (2017).
36. Gainor, J. F. et al. EGFR mutations and ALK rearrangements are associated with low response rates to PD-1 pathway blockade in non-small cell lung cancer: a retrospective analysis. *Clin. Cancer. Res.* **22**, 4585–4593 (2016).
37. Garassino, M. C. et al. Durvalumab as third-line or later treatment for advanced non-small-cell lung cancer (ATLANTIC): an open-label, single-arm, phase 2 study. *Lancet Oncol.* **19**, 521–536 (2018).
38. Lee, C. K. et al. Checkpoint inhibitors in metastatic EGFR-mutated non-small cell lung cancer—a meta-analysis. *J.Thorac. Oncol.* **12**, 403–407 (2017).

ACKNOWLEDGEMENTS
We thank Ultivue Inc. and Indica Labs for their technical support.

FUNDING INFORMATION
This work was supported by the National Natural Science Foundation of China (81871860 and 82003155), the Capital's Funds for Health Improvement and Research (2020-2-1025), and Innovation Fund for Outstanding Doctoral Candidates of Peking University Health Science Center (JH W).

AUTHOR CONTRIBUTIONS
J.W. and W.S. contributed to image analysis, data statistics, manuscript writing, and participated in the experimental design. X.Y. scanned the slides of multiplex staining and verified the PD-L1 scoring. H.W., X.L., and K.C. collected the clinical information and follow-up data of the selected cases. L.Z., X.H., and T.D. prepared the slides and performed multiplex immunofluorescence staining. L.M. and S.Z. assisted in data statistics. B.M. assisted in the implementation of the study. D.L. conceived the study, participated in its design and coordination, and helped draft and edit the manuscript.

COMPETING INTERESTS
The authors declare no competing interests.

ETHICS APPROVAL AND CONSENT TO PARTICIPATE
This study was approved by the ethics committees of the Peking University Cancer Hospital (NO. 2018KT94) and Tianjin Medical University Cancer Hospital (NO. Ek2020140). The patients' written consent was obtained and stored in Peking University Cancer Hospital and Tianjin Medical University Cancer Hospital, respectively.

ADDITIONAL INFORMATION
Supplementary information The online version contains supplementary material available at https://doi.org/10.1038/s41379-021-00903-w.

Correspondence and requests for materials should be addressed to Dongmei Lin.

Reprints and permission information is available at http://www.nature.com/reprints

Publisher's note Springer Nature remains neutral with regard to jurisdictional claims in published maps and institutional affiliations.